ELSEVIER

Journal of Fluids and Structures 21 (2005) 429–434

JOURNAL OF FLUIDS AND STRUCTURES

www.elsevier.com/locate/jfs

Special Brief Communication

On the maximum amplitude for a freely vibrating cylinder in cross-flow

J.T. Klamo, A. Leonard*, A. Roshko

Graduate Aeronautics Laboratories, California Institute of Technology, 1200 E California Blvd, Pasadena, CA 91125, USA

Received 20 May 2005; accepted 25 July 2005
Available online 4 October 2005

Abstract

The response of a freely oscillating circular cylinder (''free vibration'') in cross-flow has been studied experimentally using controlled magnetic eddy current to provide variable damping. In general, the nondimensional response amplitude, A^*, and dominant frequency, ω^*, depend on the Reynolds number, Re, and the nondimensional mass, m^*, damping, b^*, and elasticity, k^*, of the system. The main objective of this study is to characterize the maximum amplitude that is achieved for a given system as cross-flow velocity is varied. We find that this maximum amplitude, $A^*_{\max}$, occurs within a small range of values of $k^*_{\text{eff}} = -\omega^{*2}m^* + k^*$. For values of Reynolds number in the range $525 < \text{Re} < 2600$, we determine $A^*_{\max}(b^*, \text{Re})$ for lightly to moderately damped systems. Extrapolating these results to $b^* = 0$ defines limiting values of amplitude, A^*_{Lim}, which depend on Reynolds number. An important point is that these results do *not* depend on the specific value of either m^* or k^*. These results show that the Reynolds number, which has generally been ignored in discussions of maximum-amplitude data, is an important parameter.

Keywords: Vortex-induced vibrations; Reynolds number; Synchronization; Lock-in; Flow-induced oscillations

1. Introduction

The maximum amplitude in the free vibration of a structure, for us the simple case of a cylinder in cross-flow, is obviously of interest in structural engineering, but it is also an important problem in nonlinear mechanics. In classic, linear vibration the amplitude is limited only by mechanical damping in the system. However, in flow-induced vibrations the flow dynamics is coupled with that of the cylinder and the latter attains maximum amplitude in the limit of zero system damping. Defining this maximum attainable amplitude has been the subject of much experimental work, especially advanced by Griffin and collaborators [see, for example Skop and Griffin (1975) or Griffin (1980)]. In what is now often called the ''Griffin plot'', the observed amplitude is plotted against a parameter, S_G, which contains the product of the mass and damping coefficient (''mass-damping''). The objective is to determine the maximum attainable amplitude by extrapolation of the experimental values to $S_G = 0$. Almost without exception, mass-damping is not varied systematically; values of mass and damping are the ad hoc values of the particular experiment, although efforts are made to arrange for both to be as small as possible. As data from various investigators and various experiments are added, the scatter in the plot increases, raising questions as to whether the mass should be lumped together with the

*Corresponding author. Tel.: +1 626 395 4426; fax: +1 626 577 9646.
E-mail address: tony@galcit.caltech.edu (A. Leonard).

0889-9746/$ - see front matter © 2005 Elsevier Ltd. All rights reserved.
doi:10.1016/j.jfluidstructs.2005.07.010

damping [for example, see discussion in Williamson and Govardhan (2004)] and whether other parameters are playing a role. In particular, in those and most studies of flow-induced vibrations, the Reynolds number has generally been ignored. Some recent studies have begun to focus on Reynolds number effects; for instance Ryan et al. (2005) explored such effects associated with the "critical mass ratio", which was identified by Govardhan and Williamson (2002). In this Special Brief Communication, we address the effect of Reynolds number on the maximum attainable amplitude.

2. Theoretical development

The canonical arrangement for the study of vortex-induced vibrations (VIV) has been the elastically mounted circular cylinder in cross-flow that is restricted to motion only in the transverse direction. Consider such a system with mass m, damping b, and elasticity k. Of particular interest is the response of the system, characterized by the nondimensional amplitude, A^*, and frequency, ω^*, defined as

$$A^* = \frac{A}{D}, \quad \omega^* = \omega \frac{D}{U}, \tag{1}$$

where D is the cylinder diameter and U the free stream velocity. We pay particular attention to the maximum amplitude, $A^*_{\max}$, that the given systems attain.

For such an arrangement, one can obtain a nondimensionalized governing equation of motion for $y* = y/D$ as follows (Shiels et al., 2001):

$$m^* \ddot{y}^* + b^* \dot{y}^* + k^* y^* = C_L(t^*), \tag{2}$$

where

$$m^* = \frac{m}{\frac{1}{2}\rho L D^2}, \quad b^* = \frac{b}{\frac{1}{2}\rho L D U}, \quad k^* = \frac{k}{\frac{1}{2}\rho L U^2},$$
$$C_L(t^*) = \frac{F_L(t^*)}{\frac{1}{2}\rho L D U^2}, \quad t^* = t\frac{U}{D} \tag{3}$$

by using the fluid properties, free stream velocity, and cylinder diameter and length. It should also be noted that m^* in this formulation differs slightly from the traditional $m/\frac{1}{4}\pi\rho L D^2$ definition and that the damping, b^*, is related to damping in the traditional formulation by

$$b^* = \frac{2}{U_R} m^* \zeta, \tag{4}$$

where

$$U_R = \frac{U}{\omega_N D}, \quad \zeta = \frac{b}{2\sqrt{km}}, \tag{5}$$

and ω_N is the natural frequency of the system in air; U_R the reduced velocity.

For a stationary cylinder, one has

$$A^* = 0,$$
$$\omega^* = \omega^*(\mathrm{Re}) = 2\pi \mathrm{St}(\mathrm{Re}), \tag{6}$$

where there is no amplitude response since the cylinder is fixed and the frequency response is taken to be the frequency of the wake (frequency at which vortices are shed). This frequency is the well-known Strouhal frequency and is only a function of the Reynolds number of the flow. For a cylinder that is allowed to oscillate normal to the flow direction, three more parameters must be considered, so that we expect

$$A^* = A^*(m^*, b^*, k^*, \mathrm{Re}),$$
$$\omega^* = \omega^*(m^*, b^*, k^*, \mathrm{Re}), \tag{7}$$

where the frequency response is now the oscillation frequency of the cylinder.

If one assumes sinusoidal motion for a first approximation, the governing equation produces the following relation between the amplitude of the lift coefficient ($C_{L,o}$) and other parameters discussed above:

$$(k^*_{\mathrm{eff}} + \mathrm{i}\omega^* b^*) A^* = C_{L,o}, \tag{8}$$

where

$$k^*_{\text{eff}} = -\omega^{*2} m^* + k^*. \tag{9}$$

This led to the proposal by Shiels et al. (2001) that the mass and stiffness of the system can be combined into a single parameter, k^*_{eff}, the effective stiffness of the system. This potentially simplifies the response behavior as follows:

$$\begin{aligned} A^* &= A^*(k^*_{\text{eff}}, b^*, \text{Re}), \\ \omega^* &= \omega^*(k^*_{\text{eff}}, b^*, \text{Re}), \end{aligned} \tag{10}$$

whereas in the traditional formulation there are four independent parameters (U_R, ζ, m^*, Re).

The main objective of this study is to experimentally determine the function A^*_{max}, introduced by Klamo et al. (2004), and defined as

$$A^*_{\text{max}}(b^*, \text{Re}) \equiv \max_{k^*_{\text{eff}}} A^*(k^*_{\text{eff}}, b^*, \text{Re}) \tag{11}$$

for a range of Reynolds numbers, i.e. to generalize the Griffin plot.

3. Experimental results

All experiments were conducted in a free-surface low-speed water tunnel facility with test-section dimensions of 45.7 cm wide by 58.4 cm deep and tunnel speeds of 4.0–25.0 cm/s. During the course of each test, the water temperature was $20 \pm 1\,^{\circ}\text{C}$, corresponding to a kinematic viscosity of $1.004 \times 10^{-6} \pm 0.030 \times 10^{-6}\,\text{m}^2/\text{s}$. This resulted in variations in Reynolds number during tests ranging from $\text{Re} = 525 \pm 15$ to 2600 ± 75. The circular test cylinders had diameters of 10 and 38 mm. The system mass varied between 1.85 and 3.70 kg and the stiffness between 15 and 265 N/m. In this investigation we only consider high aspect ratio systems $L/D > 10$ with minimal end effects.

For a given system with certain m, b, k, and D values, a test run was completed by spanning the range of velocities of interest four times, twice in increasing and twice in decreasing increments. This was done to look for hysteresis effects

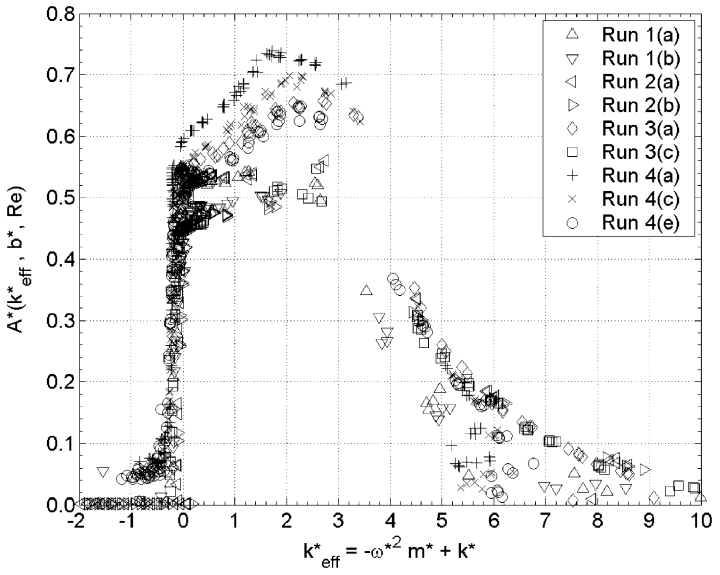

Fig. 1. Amplitude, A^*, dependence on the effective stiffness, k^*_{eff}, for various mechanical system parameters and Reynolds number. *Sequence 1*: $D = 10\,\text{mm}$, $m = 1.85\,\text{kg}$, $k = 65\,\text{N/m}$, $m^* = 78.3$, $\text{Re}|_{A^*_{\text{max}}} = 525$, $\zeta = 0.0008$ [Run 1(a)] and $\zeta = 0.0017$ [Run 1(b)]. *Sequence 2*: $D = 10\,\text{mm}$, $m = 3.70\,\text{kg}$, $k = 134\,\text{N/m}$, $m^* = 156.7$, $Re|_{A^*_{\text{max}}} = 525$, $\zeta = 0.0005$ [Run 2(a)] and $\zeta = 0.0011$ [Run 2(b)]. *Sequence 3*: $D = 10\,\text{mm}$, $m = 1.85\,\text{kg}$, $k = 265\,\text{N/m}$, $m^* = 78.3$, $Re|_{A^*_{\text{max}}} = 1000$, $\zeta = 0.0006$ [Run 3(a)] and $\zeta = 0.0026$ [Run 3(c)]. *Sequence 4*: $D = 38\,\text{mm}$, $m = 2.39\,\text{kg}$, $k = 15\,\text{N/m}$, $m^* = 7.1$, $Re|_{A^*_{\text{max}}} = 2600$, $\zeta = 0.0014$ [Run 4(a)], $\zeta = 0.0107$ [Run 4(c)], and $\zeta = 0.0211$ [Run 4(e)].

and to gauge repeatability. From such a test run the maximum amplitude for that specific system was determined. As U is varied, all nondimensional parameters except m^* will vary. However, as long as $k>0$, all values of k^*_{eff} of interest will be spanned by such a test run. This procedure was then repeated multiple times on the same system but with different values of damping. These repeated test runs at various b values then encompass a test sequence. Controlled damping values for the system were made possible by the use of a variable magnetic eddy-current (VMEC) damping system, inspired by the basic system built by Smith (1962) and used by Feng (1968) in his study of VIV. During this study, the VMEC damping system was used to impose external damping values of up to 1.25 kg/s. Typical results from multiple test sequences for various damping values are shown in Fig. 1, where the independent parameter is the effective stiffness. We denote the value of effective stiffness at peak amplitude as $k^*_{\text{eff}}|_{\max}$. Note that the peak amplitude in each case occurs around $k^*_{\text{eff}}|_{\max}\sim 1-3$, while k^*_{eff} varies from -5 to 15 in a typical experiment. In fact, we find that for lightly to moderately damped systems, the location of the maximum amplitude is invariant to individual system mass and stiffness and always occurs within the specified range of effective stiffness values, with the actual value depending only on the specific damping and Reynolds number. $A^*_{\max}$ will always occur in this range of k^*_{eff}. We note that the maximum does not occur at $k^*_{\text{eff}}=0$ (which corresponds to the synchronization condition, $\omega^{*2}=k^*/m^*$) but at a higher positive value.

Although each point that is part of a given test run in Fig. 1 corresponds to a different tunnel speed and thus a different Reynolds number and b^* value, each value of k^*_{eff} shared within a test sequence (except k^*_{eff} slightly less than 0) corresponds to nearly the same tunnel speed and Reynolds number for those points. Therefore, the differences in a test sequence at $k^*_{\text{eff}}|_{\max}$ are essentially damping effects only. The simplicity of this approach is that now a constant-Reynolds-number curve can be constructed in the amplitude-damping plane by using the points that correspond to $k^*_{\text{eff}}|_{\max}$ for a given test sequence. This experimental result allows us to determine $A^*_{\max}(b^*,\text{Re})$ for a fixed Re by varying b as described above.

Fig. 2 shows the results of transferring the data from Fig. 1 into a ''generalized'' Griffin plot with Reynolds number considerations. Four test sequences were run which covered three Reynolds numbers, Re$\sim$525, $\sim$1000, and $\sim$2600. The vertical bars associated with individual data points represent the range which captures 95% of the observed time-varying oscillation amplitudes. The effect of Reynolds number is clearly demonstrated.

Another important result of the present formulation is that mass is not an independent parameter but, rather, is implicitly contained within the effective stiffness. Therefore, theoretically only one case needs to be run for each constant-Reynolds-number curve because different values of m^* will still conform to this curve. To validate this assertion, two curves in the damping plane with two different masses, one twice as massive as the first were generated for the same Reynolds number. As can be seen in Fig. 2, the two sets of data for Re$\sim$525 corresponding to the two different mass systems show little dependence on the actual system mass.

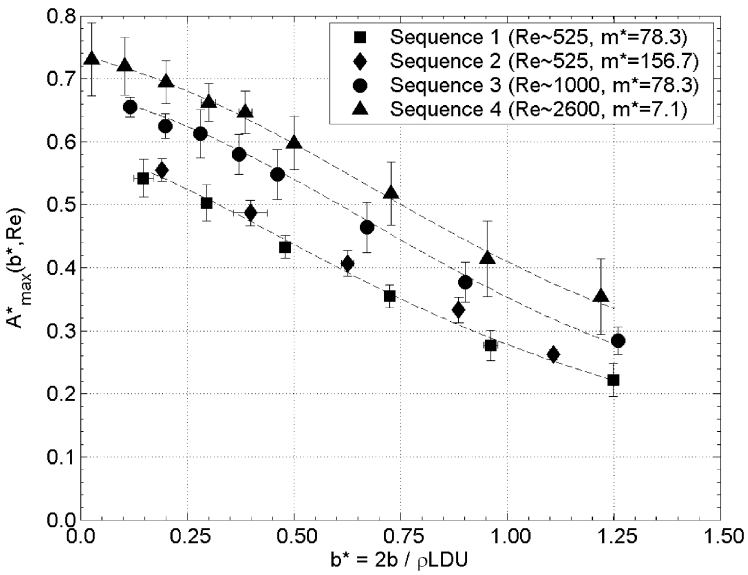

Fig. 2. New ''Generalized'' Griffin plot showing maximum amplitude, $A^*_{\max}$, dependence on b^* and Reynolds number. System parameters previously defined in Fig. 1. Horizontal bars represent the uncertainty in the measured damping value of the system.

The limiting maximum amplitude, A^*_{Lim}, that occurs in the limit of zero damping at each Reynolds number can be written simply as

$$A^*_{\mathrm{Lim}}(\mathrm{Re}) = A^*_{\mathrm{max}}(b^* \to 0, \mathrm{Re}) \tag{12}$$

and stresses the importance of Reynolds number. To exhibit such a Reynolds number effect, to a first approximation, we plot the extrapolated limiting maximum amplitudes in Fig. 3(a), fitted with a linear trend line, for the four test sequences presented in Fig. 2. These values were determined by calculating the least-squares-linear fit of the three lightest damped points for each test sequence and then extrapolating to zero damping. We also show three other zero damping, A^*_{Lim}, points from computational studies.

In order to incorporate the large number of reported maximum amplitudes from the literature that cover a much broader range of Reynolds number, a second plot, Fig. 3(b) was produced that includes reported maximum amplitude values with *small*, but finite, values of damping. We only include results for which we estimate $b^* < 0.25$ so that this figure should provide a reasonable representation of what the actual A^*_{Lim} results would be. These data were tabulated in the annual review by Williamson and Govardhan (2004). We show a large uncertainty in the values of Reynolds

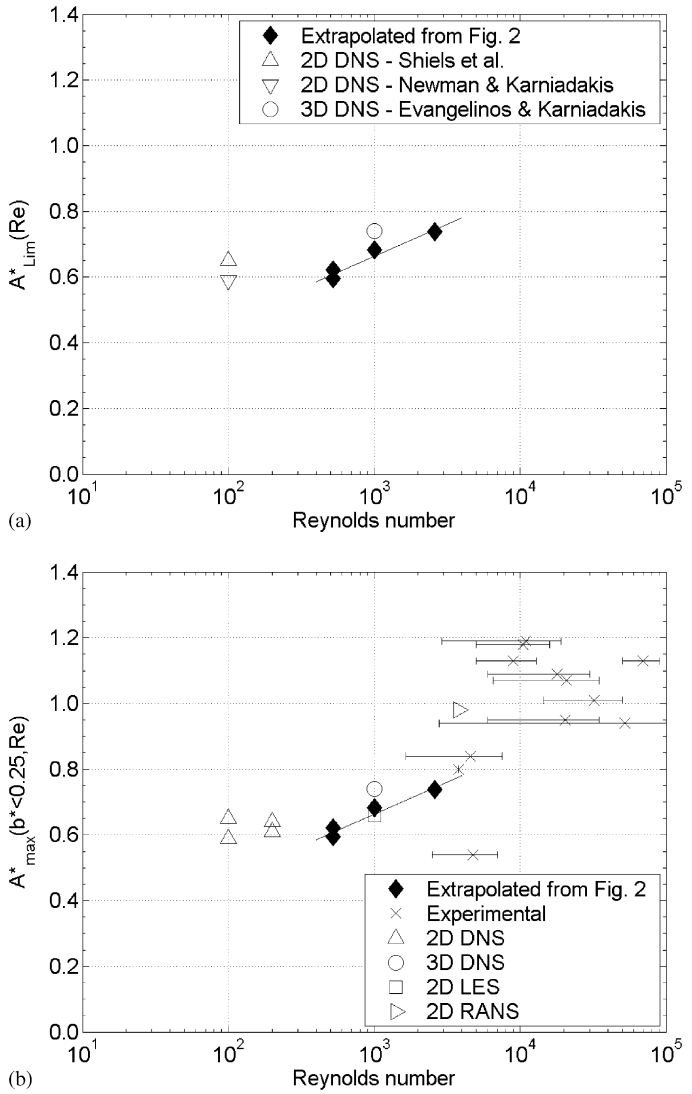

Fig. 3. Reynolds number effects on the limiting maximum amplitude. (a) Data for zero damping. (b) Comparison with data from other investigations at low damping [compiled by Williamson and Govardhan (2004)].

number that should be assigned because the value at A^*_{max} is seldom reported in the literature. Even with this uncertainty, there appears to be a strong Reynolds number effect over the entire range.

4. Conclusion

Taking advantage of the effective stiffness formulation of the parameters and introducing controllable damping, by a variable magnetic eddy-current (VMEC) damping system, it was possible in our experiments to examine the dependence of vibration amplitude on our damping parameter b^* at nearly constant Reynolds number. It was demonstrated that maximum amplitudes, A^*_{max}, depend not only on damping but also on Reynolds number. That is, instead of fitting a universal curve in the traditional Griffin plot, our data segregate onto constant-Reynolds-number curves. Also consistent with the new formulation, there is no dependence on the mass-ratio parameter, m^*. The dependence of maximum amplitude on damping could easily be extrapolated to zero damping, resulting in limiting values, A^*_{Lim}, as a function of Reynolds number. A plot of our values for zero damping, together with those from other experiments at small values of damping and using estimated values of Reynolds number for the latter, indicates that there is an important dependence of the limiting values on Reynolds number, and that more work is needed to refine and fill in the complete behavior.

Acknowledgements

Thanks to Prof. Morteza Gharib for his involvement throughout this research effort. We gratefully acknowledge the financial support provided by ONR Grant # N00014-94-1-0793. Scholarship support was provided by the National Science Foundation graduate fellowship program.

References

Feng, C.C., 1968. The measurement of vortex induced effects in flow past stationary and oscillating circular and D-section cylinders. M.A. Sc. Thesis, University of British Columbia, Vancouver, Canada.

Govardhan, R., Williamson, C.H.K., 2002. Resonance forever: existence of a critical mass and an infinite regime of resonance in vortex-induced vibration. Journal of Fluid Mechanics 473, 147–166.

Griffin, O.M., 1980. Vortex-excited cross-flow vibrations of a single cylindrical tube. ASME Journal of Pressure Vessel Technology 102, 158–166.

Klamo, J.T., Leonard, A., Roshko, A., 2004. On the maximum amplitude in vortex-induced vibrations. Bulletin of the American Physical Society 49 (9), 36.

Ryan, K., Thompson, M.C., Hourigan, K., 2005. Variation in the critical mass ratio of a freely oscillating cylinder as a function of Reynolds number. Physics of Fluids 17, 038106 (4pp.).

Shiels, D., Leonard, A., Roshko, A., 2001. Flow-induced vibration of a circular cylinder at limiting structural parameters. Journal of Fluids and Structures 15, 3–21.

Skop, R.A., Griffin, O.M., 1975. On a theory for the vortex-excited oscillations of flexible cylindrical structures. Journal of Sound and Vibration 41, 263–274.

Smith, J.D., 1962. An experimental study of the aeroelastic instability of rectangular cylinders. M.A. Sc. Thesis, University of British Columbia, Vancouver, Canada.

Williamson, C.H.K., Govardhan, R., 2004. Vortex-induced vibrations. Annual Review of Fluid Mechanics 36, 413–455.